Heart Vessels (2016) 31:1370–1379
DOI 10.1007/s00380-015-0781-y

ORIGINAL ARTICLE

Increased mortality and aggravation of heart failure in liver X receptor-α knockout mice after myocardial infarction

Xiaoqiang Liu[1] · Jianshu Gao[2] · Qiang Xia[3] · Tianfei Lu[3] · Fang Wang[1]

Received: 7 July 2015 / Accepted: 2 December 2015 / Published online: 11 January 2016
© Springer Japan 2016

Abstract Liver X receptors, LXRα (NR1H3) and LXRβ (NR1H2), are best known as nuclear oxysterol receptors and physiological master regulators of lipid and cholesterol metabolism. LXRα play a protective role in acute myocardial ischemia/reperfusion (MI/R) injury, but its role in myocardial infarction (MI) is unknown. The present study was undertaken to determine the effect of LXRα knockout on survival and development of chronic heart failure after MI. Wild-type (WT) and LXRα$^{-/-}$ mice were subjected to MI followed by serial echocardiographic and histological assessments. Greater myocyte apoptosis and inflammation within the infarcted zones were found in LXRα$^{-/-}$ group at 3 days after MI. At 4 weeks post-MI, LXRα$^{-/-}$ MI murine hearts demonstrated significantly increased infarct size, reduced ejection fraction (LXRα$^{-/-}$ 29.4 % versus WT 34.4 %), aggravated left ventricular (LV) chamber dilation, enhanced fibrosis and reduced angiogenesis. In addition, LXRα$^{-/-}$ mice had increased mortality compared with WT mice. LXRα deficiency increases mortality, aggravates pathological injury and LV remodeling induced by MI. Drugs specifically targeting LXRα may be promising in the treatment of MI.

Keywords Nuclear receptors · Myocardial infarction · Heart failure · Mortality · Apoptosis

Introduction

Acute myocardial infarction is a leading cause of morbidity and mortality worldwide [1, 2]. Heart failure is an increasing global public health problem, with the most common cause currently being cardiac remodeling after myocardial infarction (MI) [3, 4]. Thus, how to attenuate the loss of myocytes in the adverse pathological left ventricular (LV) remodeling, which includes dilatation of the ventricle and increased interstitial fibrosis [5], has long been focused on to develop an efficient strategy to improve post-infarct prognosis.

Nuclear receptors (NRs) are master regulators of transcriptional programs that integrate the homeostatic control of almost all biological processes. Liver X Receptors, LXRα (NR1H3) and LXRβ (NR1H2), are best known as nuclear oxysterol receptors and physiological regulators of lipid and cholesterol metabolism that also act in an anti-inflammatory way [6]. Recent evidence has suggested that LXRα and LXRβ are both expressed in the cardiovascular system. LXRs exert salutary effects on cardiac hypertrophy [7, 8]. The nonselective LXRα/LXRβ agonist GW3965 protects against myocardial ischemia–reperfusion (MI/R) injury [9]. Recently, it has been reported that activation of LXRα but not LXRβ subtype attenuates MI/R injury via inhibition of oxidative/nitrative stress, and subsequently reducing the apoptotic pathways mediated by

X. Liu and J. Gao contributed equally to this work.

✉ Fang Wang
onlyfang1@163.com

Tianfei Lu
lutianfei@medmail.com.cn

[1] Department of Cardiology, Shanghai General Hospital, Shanghai Jiao Tong University School of Medicine, Shanghai 200080, People's Republic of China

[2] Department of Cardiology, Yancheng First People's Hospital, The Fourth Affiliated Hospital of Nantong University, Yancheng 224006, Jiangsu, People's Republic of China

[3] Department of Transplantation and Hepatic Surgery, Ren Ji Hospital, Shanghai Jiao Tong University School of Medicine, Shanghai 200127, People's Republic of China

endoplasmic-reticulum (ER) stress and mitochondria [10]. However, the particular roles of individual LXR subtypes in the regulation of LV remodeling after MI remain unknown. Whether LXRα has therapeutic potential after MI is not clear.

In the present study, LXRα was hypothesized to attenuate the development of chronic heart failure following MI in mice. If this hypothesis was accurate, deficiency of LXRα in mice would be found altering long-term mortality as well as aggravating levels of clinical and biochemical markers of congestive heart failure after MI.

Materials and methods

Experimental animals

This investigation conforms to the National Institutes of Health Guidelines on the Use of Laboratory Animals and was approved by the Institute's Animal Ethics Committee. LXRα-deficient and wild-type (WT) C57BL/6 male mice (22–25 g) were obtained from the Jackson Laboratories (Bar Harbor, ME, USA) and were housed at 25 ± 5 °C, adherent to a 12 h light–dark cycle, with food and water freely available.

Surgical generation of MI model

Myocardial infarction procedures were performed utilizing a novel method as described in previous study [11]. In brief, mice were anesthetized with 2 % isoflurane inhalation with an isoflurane delivery system but not ventilated. A small skin cut (1.2 cm) was made over the left chest, and a purse suture was done. By dissecting and retracting of the pectoral major and minor muscles, the fourth intercostal space was exposed to make a small hole in it with a mosquito clamp to open the pleural membrane and pericardium. With the clamp slightly open, the murine heart was smoothly and gently "popped out" through the hole. The left anterior descending coronary artery (LCA) was located, sutured, and ligated at a site ≈3 mm from its origin using a 6–0 silk suture. The ligation was deemed successful when the anterior wall of the LV turned pale. When ligation was completed, the heart was immediately placed back into the intrathoracic space followed by manual evacuation of air and closure of muscles and the skin, by means of the previously placed purse-string suture. The mouse was then allowed to breathe room air and monitored during the recovery period, which generally lasted 3–5 min. Sham-operated animals were subjected to identical surgical procedures, except that the suture passed beneath the LCA was not tied. After recovery from surgery, the mice were returned to under standard animal housing conditions.

Assessment of infarct size and survival

Myocardial infarction size was determined by the use of 2,3,5-triphenyltetrazolium chloride (TTC) as described elsewhere [12]. In brief, 28 days after surgery hearts from randomly chosen mice were removed, frozen at −20 °C and sliced into ~1 mm thick sections perpendicular to the long axis of the heart using a heart slice chamber. These murine hearts were used to determine infarct size only. TTC staining was performed and slices were photographed with a digital camera. The survival analysis was performed in sham-operated WT/LXRαKO ($n = 15$), WT-MI ($n = 25$) and LXRαKO-MI ($n = 21$). During the study period of up to 4 weeks, cages were inspected twice a day and dead animals were immediately subjected to examination for the presence of MI.

Echocardiographic measurements

In vivo cardiac function was determined by echocardiography at 24 h and 4 weeks after MI. Mice were anesthetized with 1.5 % isoflurane. Transthoracic two-dimensional echocardiographic views of the mid-ventricular short axis were obtained at the level of the papillary muscle tips below the mitral valve (Vevo 2100, VisualSonic, Toronto, Canada). LV diameter was measured and subsequently fractional shortening (FS% = [(LVEDD − LVESD)/LVEDD) × 100]) and left ventricular ejection fraction (LVEF) were calculated. An individual blinded to the experimental groups recorded the cardiac structural parameters which were read to calculate the functional parameters of the heart by a second individual.

Terminal deoxynucleotidyl transferase-mediated 29-deoxyuridine 59-triphosphate nick-end labeling assay (TUNEL)

Apoptotic cells in formalin-fixed, paraffin-embedded murine heart tissue sections were identified with ApopTag Fluorescein In Situ Apoptosis Detection Kit S7110 (Chemicon International), according to the manufacturer's protocol. Cells with nuclear positive staining by fluorescent antibodies for DNA fragmentation were visualized directly under a fluorescence microscope and counted (original magnification 200×). At least 3 fields per section were examined, as described previously [13].

Histological analysis

All morphometric analyses were performed in a standard manner on 5 transverse sections of each murine heart. Tissue sections were stained with hematoxylin and eosin and Masson's trichrome or used for immunohistochemistry as

previously described [14]. Cardiac fibroblasts were plated on fibronectin-precoated chamber slides, fixed, and incubated with rhodamine-conjugated phalloidin and a specific antibody to a-smooth muscle actin (a-SMA).

Immunofluorescence

After incubation with primary antibodies to CD31 (1/50, GB13063, Wuhan goodbio technology CO., Wuhan, China) overnight at 4 °C, the paraffin-embedded heart sections were washed with PBS three times and incubated with cyanin 3 (Cy3) conjugated secondary donkey anti-goat IgG (1/300, 705-165-003, Wuhan goodbio technology CO., LTD, Wuhan, China) for 1 h at room temperature in a darkened humidified chamber. The final preparations were washed with PBS and mounted with fluorescent mounting medium containing 4′, 6-diamidino-2-phenylindole (DAPI) (C1002, Beyotime Institute of Biotechnology, Shanghai, China). Each section was observed under a confocal laser scanning microscope at a magnification of 200× and 400×.

Western blot analysis

The harvested hearts were homogenized and lysed with cell lysis buffer which containing 1 protease inhibitor cocktail tablet per 10 mL of Lysis Reagents (Complete; Roche, Indianapolis, IN, USA). Total protein extracts, after centrifugation at 12,000*g* at 4 °C for 30 min, were mixed with loading buffer and heated at 99 °C for 5 min. Protein concentrations were determined with a bicinchoninic acid (BCA) protein assay kit (Beyotime Biotechnology, China). For western blot analysis an equal amount of protein (60 mg) was loaded in each well and subjected to 12 % sodium dodecylsulfate-polyacrylamide gel electrophoresis (SDS-PAGE). Separated proteins were then transferred from the gel to nitrocellulose membranes (Whatman) and blocked with LI-COR blocking buffer for 1–2 h. The membranes were incubated with the primary antibodies overnight at 4 °C. The primary antibodies were as follows: LXRα (1:1000 ab41902, abcam), caspase-3 (1:1000 #9664, Cell Signaling Technologies, inc.), p-AKT (1:1000 #4060, Cell Signaling Technologies, inc.), GAPDH (1:1000 #2118, Cell Signaling Technologies, inc.). Following washing primary antibodies with TBS/0.05 % Tween-20 thrice, the membranes were incubated with appropriate secondary antibodies (1:10,000, LI-COR Biosciences) for 1–2 h at room temperature and then washed again in TBS/0.05 % Tween-20 for 3 times. The blot was visualized using an Odyssey infrared imaging system (LI-COR Biosciences). Samples were corrected for background and quantified by Odyssey software. All values were normalized to the loading control and expressed as fold increase relative to control.

Real-time quantitative PCR

Total RNA was isolated from tissues and cardiomyocytes with TRIzol Reagent and purified with Qiagen's RNeasy Mini Kit (Qiagen). Reverse transcription was performed by Omniscript RT Kit (Qiagen). The resultant cDNA was amplified by SYBR® Premix Ex Taq™ Perfect Real Time Kit (Takara BIO, Otsu, Japan). The PCR reaction was directly monitored by The LightCycler® 480 Real Time PCR System (Roche Applied Science, Indianapolis, IN, USA). Utilized SYBR Green real-time PCR primers were as follows: mouse GAPDH forward 5′-TCACTGCCACCCAGAAGA-3′ and reverse 5′-GACGGACACATTGGGGGTAG-3′; mouse LXRα forward 5′-GCTCATTGCCATCAGCATC-3′ and reverse 5′-AGCATCCGTGGGAACATCA-3′; mouse TNF-a forward 5′-TCGTAGCAAACCACCAAGTG-3′ and reverse 5′-AGATAGCAAATCGGCTGACG-3′; mouse IL-6 forward 5′-GTCACAGAAGGAGTGGCTAAG-3′ and reverse 5′-TTCTGACCACAGTGAGGAATG-3′; mouse IL-1β forward 5′-TGGAGAGTGTGGATCCCAAGCAAT-3′ and reverse 5′-TGCTTGTGAGGTGCTGATGTACCA-3′; mouse Collagen forward 5′-AAG GTT CTC CTG GTG AAG CTG GT-3′ and reverse 5′-CTG AGC TCC AGC TTC TCC ATC TT-3′; mouse MMP9 forward 5′-GCT GAC TAC GAT AAG GAC GGC A-3′ and reverse 5′-TAG TGG TGC AGG CAG AGT AGG A-3′. Real-time PCR data were represented as Ct values, defined as the crossing threshold of PCR, obtained via LightCycler 480 Data Analysis software. Relative mRNA expression levels of the samples were calculated as described, and expressed as $2^{-\Delta\Delta Ct}$ [10]. Data were standardized by GAPDH.

Statistical analysis

All values were expressed as mean ± SEM. Comparison of survival was performed from Kaplan–Meier plots followed by log-rank test. Comparisons between two parameters were analyzed by the unpaired Student's *t* test. Statistical analyses between more than 3 groups were performed by 1-way ANOVA. Significance was set at $P < 0.05$.

Results

Upregulation of LXRα at the infarction site

To assess the importance of LXRα in the cardiac healing process, we first examined the diversification of LXRα gene expression in the infarct regions of the hearts from WT post-MI mice. Elevated expression of LXRα was found in the infarct region compared with sham-operated heart

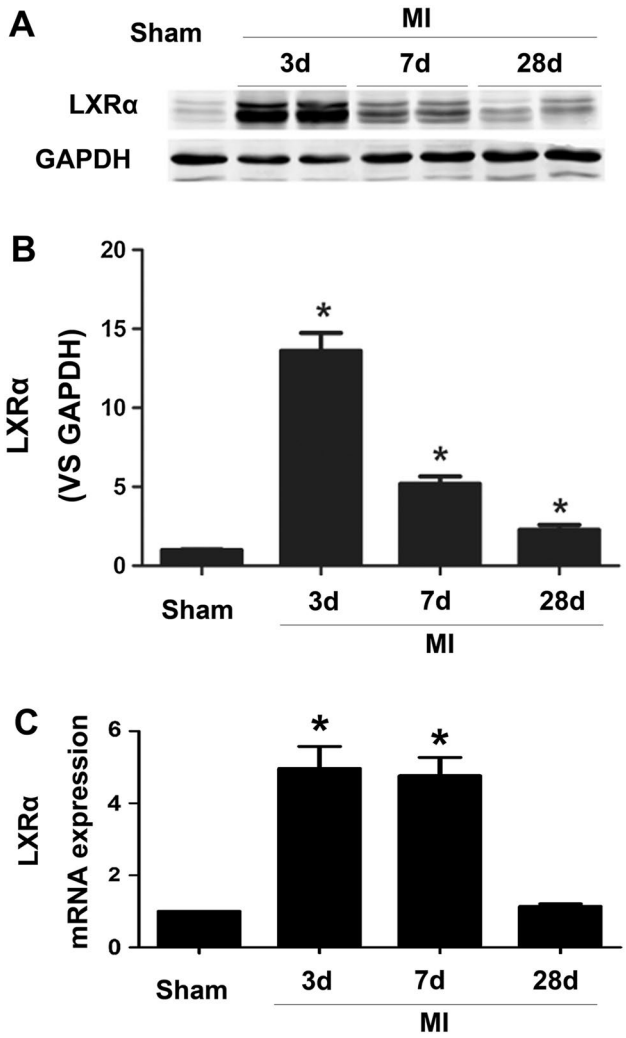

Fig. 1 LXRα expression is upregulated after MI. **a** Typical Western blot showing LXRα expression in the infarct region of sham-operated and infarcted WT mice on the indicated days after MI. **b** Quantitative analyses of the relative levels of protein expression. **c** Expression of LXRα mRNA detected by real-time quantitative PCR in the infarct areas at the indicated days after MI. Sham-operated animals served as control. Results were normalized against GAPDH and converted to fold induction relative to sham-operated controls. There were 4–5 mice in each group and data were expressed as mean ± SEM. *$P < 0.05$ versus sham-operated controls

as demonstrated by both Western blot and real-time PCR. LXRα expression peaked at day 3 and gradually declined but persisted up to day 28 after MI (Fig. 1).

Mortality

Mortality rates over the 4-week observation period were higher in LXRα knockout mice with MI than in infarcted

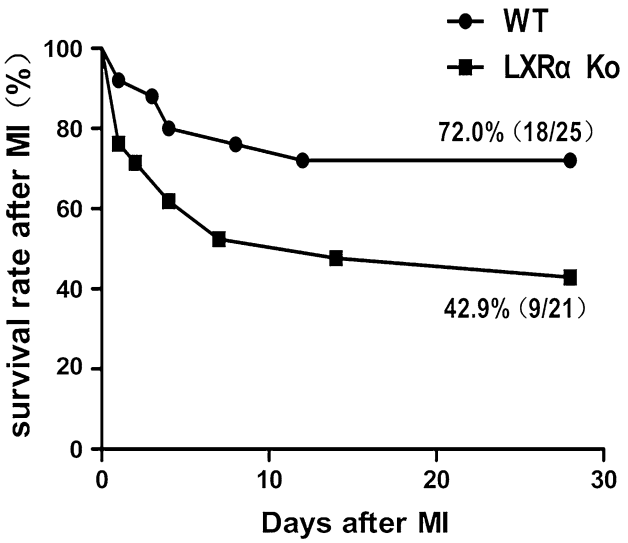

Fig. 2 Increased mortality rates after MI in LXRα$^{-/-}$ mice. Mortality was negligible in sham-operated mice and increased in both genotypes after MI over entire 4-week observation period. Mortality rates were higher in group of infarcted LXRαKO mice than in WT mice with MI (log-rank $P = 0.0453$)

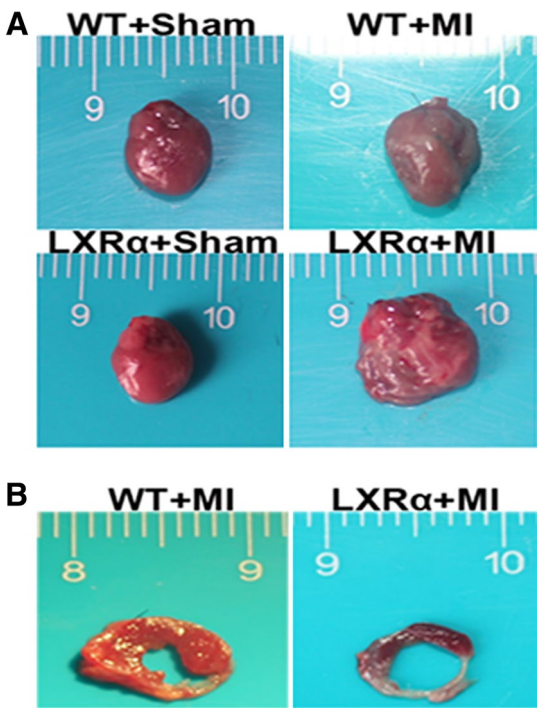

Fig. 3 Cardiac structure is impaired in LXRα$^{-/-}$ mice following MI. **a** Representative images taken at 4 weeks post-MI demonstrate impaired LV wall integrity in LXRα$^{-/-}$ hearts. **b** TTC staining performed on 28 day post-MI hearts revealed infarct size is significantly greater in LXRα$^{-/-}$ than WT mice

Table 1 Echocardiographic parameters of WT and LXRa$^{-/-}$ mice 1 day post-MI

	WT + Sham ($n = 10$)	LXRa$^{-/-}$ + Sham ($n = 10$)	WT + MI ($n = 20$)	LXRa$^{-/-}$ + MI ($n = 16$)
EF %	62.28 ± 1.31	60.66 ± 1.49	40.56 ± 1.46*	37.37 ± 2.32$^{\#}$
FS %	31.93 ± 1.33	30.45 ± 1.37	22.80 ± 0.98*	21.62 ± 1.12$^{\#}$
LVEDD (mm)	3.16 ± 0.11	3.21 ± 0.12	3.54 ± 0.09*	3.63 ± 0.10$^{\#}$
LVESD (mm)	2.13 ± 0.11	2.27 ± 0.12	2.63 ± 0.08*	2.73 ± 0.11$^{\#}$

EF ejection fraction, *%FS* percent fractional shortening, *LVEDD* LV end-diastolic diameter, *LVESD* LV end-systolic diameter

* $P < 0.05$, WT + MI versus WT + sham; $^{\#}$ $P < 0.05$, LXRa$^{-/-}$ + MI versus LXRa$^{-/-}$ + Sham

Table 2 Echocardiographic parameters of WT and LXRa$^{-/-}$ mice 28 days post-MI

	WT + Sham ($n = 10$)	LXRa$^{-/-}$ + Sham ($n = 10$)	WT + MI ($n = 16$)	LXRa$^{-/-}$ + MI ($n = 10$)
EF %	68.23 ± 1.11	66.87 ± 1.29	34.38 ± 1.46	29.35 ± 1.86*
FS %	38.09 ± 0.93	37.27 ± 1.09	17.66 ± 0.71	15.18 ± 0.76*
LVEDD (mm)	3.51 ± 0.10	3.63 ± 0.11	4.65 ± 0.10	5.10 ± 0.13*
LVESD (mm)	2.28 ± 0.12	2.43 ± 0.13	4.15 ± 0.08	4.62 ± 0.11*

* $P < 0.05$, LXRa$^{-/-}$ + MI versus WT + MI

WT mice (LXRαKO-MI 57.1 % versus WT-MI 28.0 %; log-rank $P = 0.0453$), as shown in Fig. 2. Postmortem necropsy verified the presence of MI in all infracted animals. Survival was identical between Sham-WT and Sham-LXRα$^{-/-}$ mice. Deaths in sham-operated mice ($n = 1$ WT sham, $n = 1$ LXRαKO sham) occurred early after surgery, related to postsurgical bleeding.

Infarct size

Macroscopically, the two groups of mice had significantly larger heart volume than the sham-operated mice at 28 days post-MI. Heart shape of infarcted LXRα knockout mice became more spherical relative to that of WT mice with MI (Fig. 3a), reflecting aggravation of LV global remodeling after LXRα knockout. TTC staining of post-MI hearts at 28 days revealed apparently higher infarct/LV area ratios in LXRα$^{-/-}$ than in WT mice (Fig. 3b).

LXRα$^{-/-}$ mice exhibit cardiac dysfunction after MI

Results from survival studies showed that the majority of deaths concentrated within 1 week after MI in WT and LXRα$^{-/-}$ mice (Fig. 2), suggesting that critical cardiac events concerning structural changes occurred in the early phase of post-MI. Therefore, cardiac function was assessed using 2D and Doppler echocardiography (ECG) on mice at days 1 and 28 following MI.

ECG at 1 day after surgery revealed that mice from both LXRα$^{-/-}$ and WT groups exhibited significantly impaired cardiac function. No significant difference was observed between the two groups at this time point (Table 1). However, LXRα$^{-/-}$ mice were inferior in LV systolic function, as judged by percent ejection fraction (%EF) and fractional shortening (%FS), compared with WT mice at day 28 after MI. Furthermore, left ventricular end-systolic diameter (LVESD) and end-diastolic diameter (LVEDD) increased significantly in LXRα$^{-/-}$ mice than in WT mice at day 28 after MI (Table 2), indicating severe LV dilatation and cardiac remodeling in LXRα$^{-/-}$ mice.

Deficiency of LXRα increase MI-induced myocardial apoptosis and inflammation

Apoptotic death of cardiomyocytes has been suggested to cause LV remodeling and dysfunction [15]. Cardiomyocyte apoptosis was quantified by TUNEL assay in murine hearts 3 days after MI. The number of TUNEL-positive cardiomyocytes in the border area significantly increased in LXRα$^{-/-}$ mice than in WT mice (Fig. 4a, b). Western blot analysis showed a conspicuous elevation in cleaved caspase-3 level of LXRα$^{-/-}$ murine hearts at day 3 after MI (Fig. 4c, d). Increased phosphorylation of Akt is generally considered as an anti-apoptotic signal [16]. An increase in Akt phosphorylation was obvious in WT murine hearts at 3 days post-MI. However, Akt phosphorylation significantly decreased in the infarct LV regions of LXRα$^{-/-}$-MI versus WT-MI (Fig. 4c, e). Inflammation is the first stage of cardiac repair after myocardial infarction [17]. Therefore, we examined the expression levels of proinflammatory cytokines, such as tumor necrosis factor (TNF)-a, interleukin (IL)-6, and IL-1β, in the heart of WT mice and

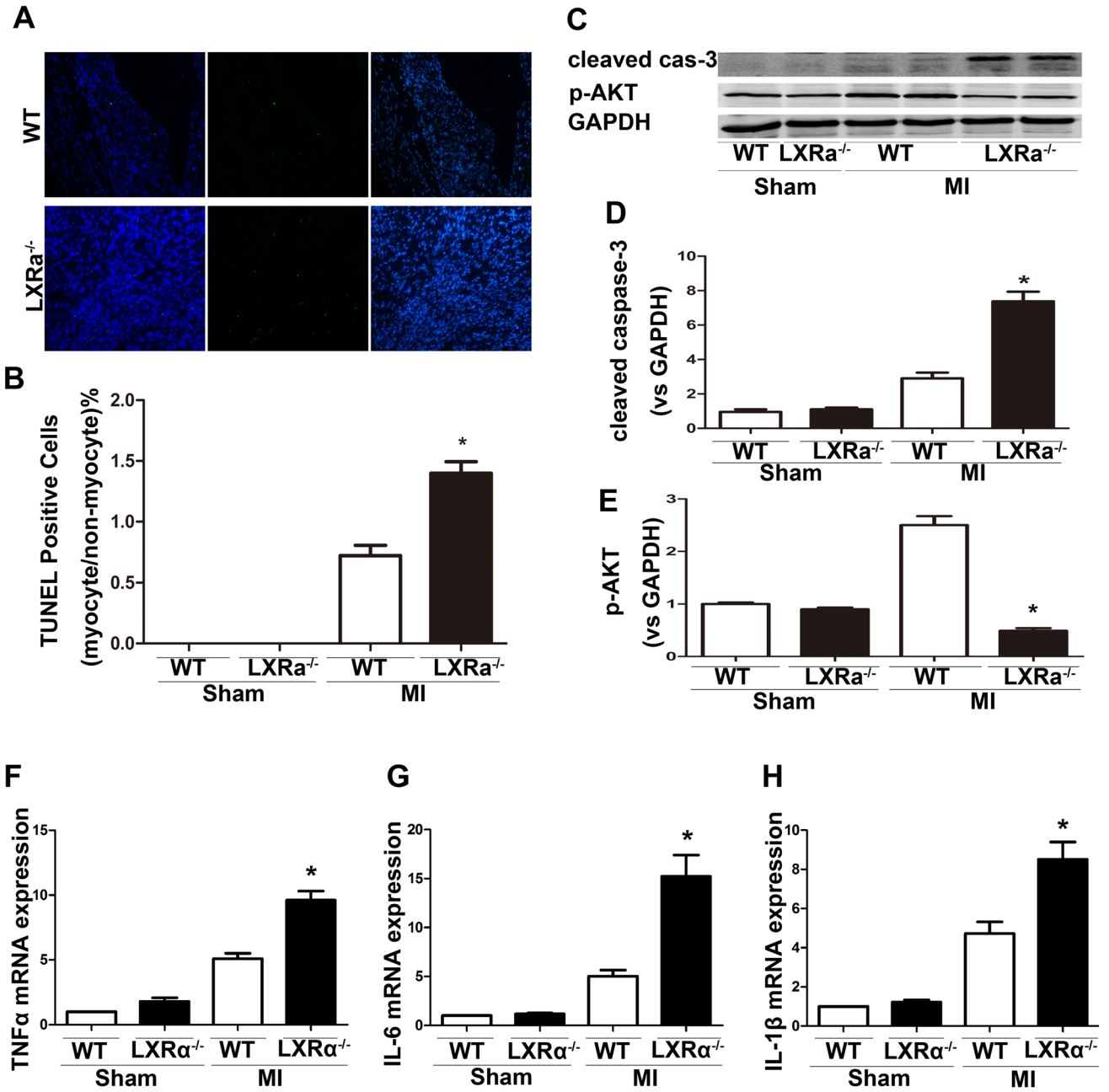

Fig. 4 LXRα deficiency results in enhanced apoptosis and inflammation post-MI. **a** TUNEL-positive myocytes (*green*) at 3 days post-MI revealed an increase in apoptosis in LXRα$^{-/-}$ mice compared to WT mice. DAPI nuclear staining in *blue* (TUNEL assay original magnification, ×200). **b** The ratio of myocyte/non-myocyte apoptosis increased at 3 days post-MI in LXRα$^{-/-}$ mice ($n = 3$ per group, 5 fields per heart). **c** Representative Western blot showing cleaved caspase-3 and phosphorylated Akt expression in the infarct region of sham-operated and infarcted WT/LXRα$^{-/-}$ mice at 3 days after MI. **d**, **e** Quantitative analyses of the relative levels of protein expression. **f–h** mRNA expression levels of proinflammatory genes detected by real-time quantitative PCR in the hearts of WT and LXRα KO mice at 3 days after MI. Sham-operated animals served as control. Results were normalized against GAPDH and converted to fold induction relative to sham-operated controls. There were 4–10 mice in each group and data were expressed as mean ± SD. *$P < 0.05$ versus WT/MI group

LXRα$^{-/-}$ mice after MI. A quantitative RT-PCR experiment revealed that these inflammatory genes had markedly increased in both WT mice and LXRα$^{-/-}$ mice 3 days post-MI when compared with their respective sham groups. Interestingly, the proinflammatory cytokines mRNA expression had a significant increase in the infarct LV regions of LXRαKo mice when compared with WT mice 3 days post-MI (Fig. 4f–h).

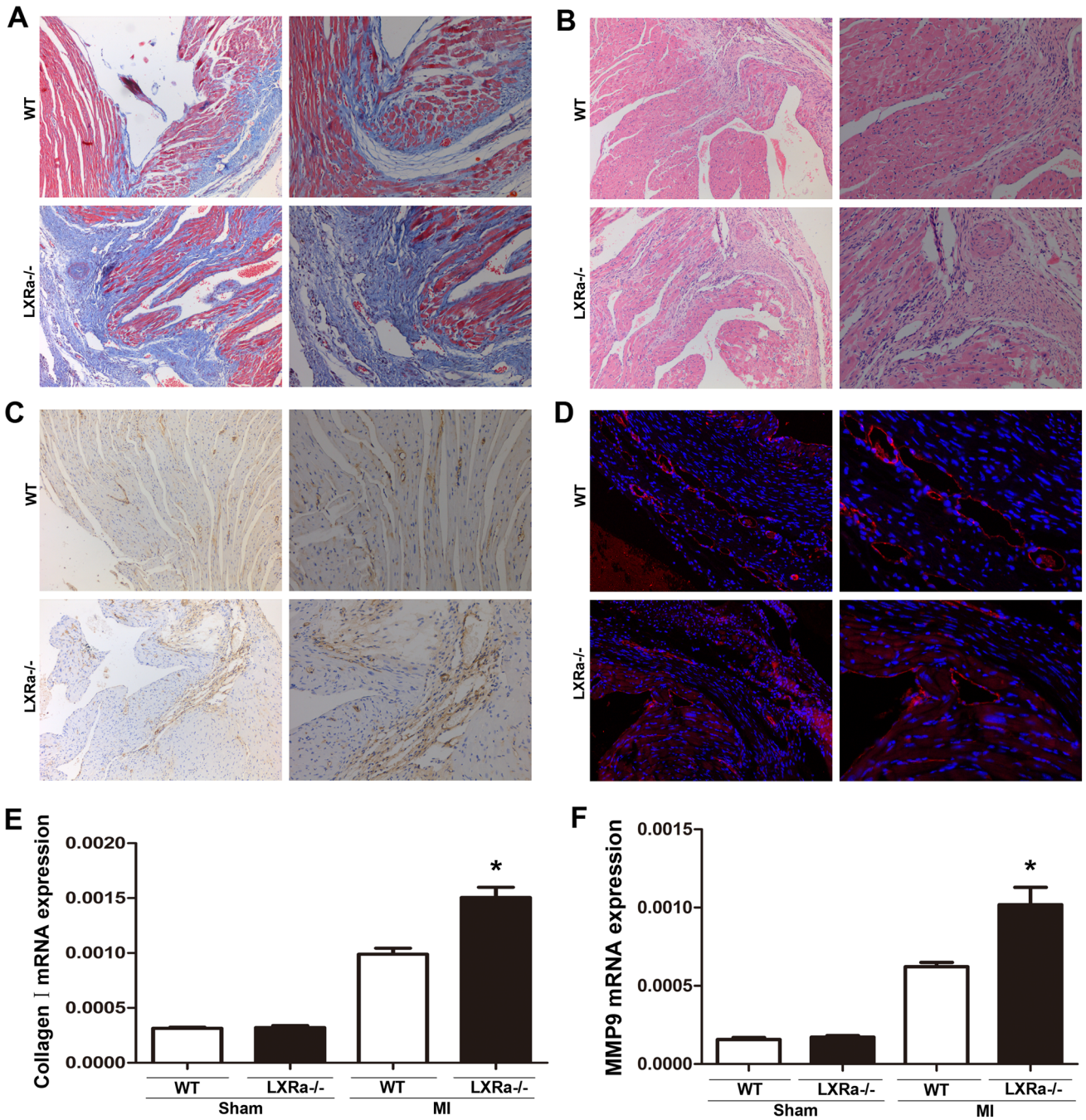

Fig. 5 LXRα deficiency results in increased fibrosis and reduction angiogenesis after MI. **a** Masson's trichrome staining to detect interstitial fibrosis in the border zone of WT and LXRα$^{-/-}$ mice at 4 weeks after MI (original magnification, ×100 and ×200). **b** Serial frozen sections were stained with hematoxylin-eosin for morphological identification of border and infarct areas (original magnification, ×100 and ×200). **c** α-SMA-stained images from the infarct LV regions of WT and LXRα$^{-/-}$ hearts post-MI (original magnification, ×100 and ×200). **d** Representative heart sections from WT and LXRα$^{-/-}$ mice harvested at 28 days after MI. Sections were stained with CD31 antibodies (original magnification, ×200 and ×400). **e**, **f** After 28 days post-MI, ventricular mRNA levels of collagen I and MMP-9 were determined by qRT-PCR and normalized to GAPDH mRNA levels. *Bars* represent group mean ± SEM (n = 5–10). *$P < 0.05$ versus WT/MI group

LXRα$^{-/-}$ mice aggravate myocardial fibrosis and reduce angiogenesis after MI

Masson's trichrome staining for interstitial fibrosis in the border zone was analyzed in WT and LXRα$^{-/-}$ murine hearts at 4 weeks after MI. Figure 5a demonstrates a significant aggravation in the fibrosis area in LXRα$^{-/-}$ MI mice than in WT MI mice. The border zone was confirmed by hematoxylin-eosin (HE) staining on serial sections (Fig. 5b). Expression of α-smooth muscle actin (α-SMA) is considered as a marker for the differentiation of fibroblasts into myofibroblasts [18]. LXRα$^{-/-}$ mice had a significant increase in number of α-SMA–positive myofibroblasts compared with WT mice in the peri-infarct areas at 4 weeks after MI (Fig. 5c). Promoted angiogenesis has been considered to facilitate myocardial recovery from ischemic injury [19, 20]. A decline in number of CD31-positive capillary vessels was found in LXRα$^{-/-}$ mice compared with WT mice at day 28 after MI (Fig. 5d). To supporting this notion, we detected collagen I and matrix metalloproteinase (MMP)-9 mRNA expression by RT-PCR analysis of infarcted murine hearts at day 28 after MI. As shown in Fig. 5e, f, the collagen I and MMP-9 mRNA expression increased post-MI compared with their respective sham groups. Furthermore, in the infarcted LV regions, LXRα$^{-/-}$ mice post-MI had a significant increase in collagen I and MMP-9 than WT mice post-MI did.

Discussion

The significant findings in the present study were that LXRα-deficient mice exhibit a higher mortality rate and exacerbated cardiac dysfunction and remodeling after MI when compared with wild-type mice. This study provides direct evidence supporting a cardioprotective role of LXRα in post-ischemic heart failure, which was mediated, at least in part, by preventing apoptosis, inflammation and fibrosis of cardiomyocytes and promotion of myocardial angiogenesis. Cardiac remodeling is generally accepted as a determinant of the clinical course of heart failure, involving functional, geometric, cellular, and molecular changes [21]. It is one of the major therapeutic challenges to reduce post-MI cardiac remodeling in modern cardiology. Drugs specifically targeting LXRα may be promising in treating ischemic heart disease.

Liver X receptors, LXRα and LXRβ (NR1H3 and NR1H2, respectively), were identified in the mid-1990s based on sequence homology with other nuclear receptors [22]. LXRα and LXRβ proteins have considerable sequence homology (approximately 77 % identity in DNA and ligand-binding domains) and are activated by the same ligands. LXRα is expressed predominantly in metabolically active tissues such as the liver, kidney, intestine, macrophages, and adipose tissue, whereas LXRβ is more ubiquitously expressed. They play a central role in the transcriptional control of lipid and cholesterol metabolism [23]. Although LXRs were initially discovered as orphan receptors, the search for its natural ligands resulted in the identification of various oxysterols as endogenous LXR agonists. These oxidized cholesterol metabolites include 24(*S*)-hydroxycholesterol, 22(*R*)-hydroxycholesterol, 27-hydroxycholesterol and 24(*S*),25-epoxycholesterol. There were a plethora of synthetic LXR agonists such as T0901317 and GW3965 were found in recent years [6]. However, almost all current LXR agonists are non-specific, and they not only activate LXRα, but also cause activation of LXRβ. It has reported that combined therapy of LXR agonist T0901317 and adipose-derived mesenchymal stem cells could improve cardiac function after MI [24]. This confirms our research from different aspects. Recent research suggests that LXRα/LXRβ are both expressed in the cardiovascular system, LXRα is selectively upregulated by ischemia/reperfusion, whereas LXRβ expression remained mostly unaffected [10]. However, another study showed that LXRβ was increased by 28 % in infarcted hearts, whereas post-infarction LXRα levels were unchanged at 24 h after MI compared to sham-operated animals [9]. Our evidence demonstrated an elevation in LXRα expression in the infarct region that peaked at day 3 and gradually declined but persisted up to day 28 post-MI. These results suggest that LXRα may play a pivotal role in the cardiac healing process after MI. The discrepancy between the two studies about the expression of LXRα may result from different time points of observation.

The major predictor of mortality is the impairment of left ventricular function after MI. Infarct size is a crucial variable for the interpretation of heart failure after MI [25]. Therefore, increased mortality in LXRα$^{-/-}$ compared with WT mice might have resulted from larger infarct sizes in LXRα$^{-/-}$ murine hearts. Exaggerated ventricular remodeling is probably linked to larger infarct sizes in LXRα$^{-/-}$ mice post-MI. Pathological left ventricular remodeling helps to preserve cardiac output in the early phase after MI. However, in the long term, this process can lead to increased oxygen consumption, deterioration of cardiac contractile function, impairment of ventricular relaxation and occurrence of arrhythmias [26]. Due to the importance of left ventricular dilatation in heart failure evolution, LVESV and LVEDV are better predictors of long-term mortality than LVEF [27]. Our experiment has exhibited an increase in LVESV and LVEDV in LXRα$^{-/-}$ mice compared with WT mice at day 28 after MI. In the present study, the majority of deaths occurred within 1 week after MI in WT and LXRα$^{-/-}$ mice. Since the most common cause of death is arrhythmias or hemodynamic

decompensation, we speculate that there is an early increase in cardiac arrhythmias and hemodynamic decompensation in LXRα$^{-/-}$ mice after MI.

Apoptosis contributes to the progression of MI, and increased apoptosis in areas remote from the infarct contributes to late LV remodeling after MI, whereas anti-apoptotic treatment at an early stage reduces the infarct size [28, 29]. In the present study, we have found that deletion of the LXRα gene increases cardiomyocyte apoptosis and cleaved caspase-3, and decreases activation of anti-apoptotic kinase p-Akt at 3 days post-MI. Expression levels of several inflammatory genes, such as TNF-a, IL-6 and IL-1β, were increased in WT and LXRα KO mice 3 days after MI. The degree of increase was higher in LXRα KO mice than in WT mice. As inflammatory cytokines are reported to induce cardiomyocyte apoptosis [30], it is possible that the enhanced apoptosis in the infarct area LXRα KO mice is caused in part by the increased inflammatory.

Cardiac fibroblasts are largely responsible for forming the infarct scar by proliferating, differentiating to myofibroblasts, and depositing large amounts of extracellular matrix (ECM) [31]. The appearance and disappearance of myofibroblasts should be right in time; if activated myofibroblasts persist too long in the myocardium, they will cause extensive scarring and fibrosis. We observed myocardial fibrosis in WT and LXRα$^{-/-}$ mice at 4 weeks post-MI. Deficiency of LXRα was found associated with aggravated myocardial fibrosis. ECM remodeling contributes to myocardial fibrosis, which is considered to be an independent risk factor in the progression of heart failure [32]. Type I collagen is the predominant component of the cardiac ECM, its synthesis and deposition lead to an increase in myocardial stiffness, eventually resulting in cardiac systolic and diastolic dysfunction [33]. The matrix metalloproteinases (MMPs) are endopeptidases that are present within the myocardium. The enhanced activity and expression of MMP-9 are associated with increased collagen formation [34]. In our experiment, mRNA expression of type I collagen and MMP9 significantly increased in LXRα$^{-/-}$ mice compared to WT mice at 4 weeks post-MI. Angiogenesis is an adaptive response to hypoxia and ischemia. Increased angiogenesis has been documented to facilitate cardiac recovery from ischemic injury [35]. Another finding in the present study is that LXRα contributes to angiogenesis after MI (Fig. 5d). Impaired angiogenesis in LXRα$^{-/-}$ mice could partly explain the aggravated cardiac dysfunction.

There are still a few limitations in the present study. We used mice harboring a systemic deletion of LXRα, but some aspects of chronic heart failure in LXRαKO mice might be due to unopposed activity of LXRβ. LXRβ regulates lipogenesis and cholesterol efflux in skeletal muscle, with anti-thrombotic effects in human platelets [36]. Considerable evidence has also identified LXRβ as anti-inflammatory transcription factors and physiological regulators of immune responses and apoptosis. Therefore, further studies are required to detect whether LXRβ deletion has similar or divergent effects on the development of heart failure.

In conclusion, the present study showed that LXRα plays an important role in cardiac remodeling by adjusting myocardial apoptosis, inflammation, fibrosis and angiogenesis. Manipulation of LXRα or LXRα-dependent signaling pathways may be promising in cardiac healing after MI.

Acknowledgments We thank Laboratory of Transplantation and Hepatic Surgery, Ren Ji Hospital. Furthermore, we are grateful for Jiang Zhang and Dawei Li for providing excellent technical assistance.

Compliance with ethical standards

Conflict of interest The authors declare no conflict of interest.

Ethical approval This investigation conforms to the National Institutes of Health Guidelines on the Use of Laboratory Animals, and was approved by the Institute's Animal Ethics Committee.

References

1. Pu J, Mintz GS, Brilakis ES, Banerjee S, Abdel-Karim AR, Maini B, Biro S, Lee JB, Stone GW, Weisz G, Maehara A (2012) In vivo characterization of coronary plaques: novel findings from comparing greyscale and virtual histology intravascular ultrasound and near-infrared spectroscopy. Eur Heart J 33:372–383
2. Zhang BH, Guo CX, Wang HX, Lu LQ, Wang YJ, Zhang LK, Du FH, Zeng XJ (2014) Cardioprotective effects of adipokine apelin on myocardial infarction. Heart Vessels 29:679–689
3. Cabiati M, Martino A, Mattii L, Caselli C, Prescimone T, Lionetti V, Morales MA, Del Ry S (2014) Adenosine receptor expression in an experimental animal model of myocardial infarction with preserved left ventricular ejection fraction. Heart Vessels 29:513–519
4. Gheorghiade M, Bonow RO (1998) Chronic heart failure in the United States: a manifestation of coronary artery disease. Circulation 97:282–289
5. Jessup M, Brozena S (2003) Heart failure. N Engl J Med 348:2007–2018
6. Jakobsson T, Treuter E, Gustafsson JA, Steffensen KR (2012) Liver X receptor biology and pharmacology: new pathways, challenges and opportunities. Trends Pharmacol Sci 33:394–404
7. Kuipers I, Li J, Vreeswijk-Baudoin I, Koster J, van der Harst P, Sillje HH, Kuipers F, van Veldhuisen DJ, van Gilst WH, de Boer RA (2010) Activation of liver X receptors with T0901317 attenuates cardiac hypertrophy in vivo. Eur J Heart Fail 12:1042–1050
8. Wu S, Yin R, Ernest R, Li Y, Zhelyabovska O, Luo J, Yang Y, Yang Q (2009) Liver X receptors are negative regulators of cardiac hypertrophy via suppressing NF-κB signalling. Cardiovasc Res 84:119–126
9. Lei P, Baysa A, Nebb HI, Valen G, Skomedal T, Osnes JB, Yang Z, Haugen F (2013) Activation of Liver X receptors in the heart leads to accumulation of intracellular lipids and attenuation of ischemia-reperfusion injury. Basic Res Cardiol 108:323
10. He Q, Pu J, Yuan A, Lau WB, Gao E, Koch WJ, Ma XL, He B (2014) Activation of liver-X-receptor alpha but not

liver-X-receptor beta protects against myocardial ischemia/reperfusion injury. Circ Heart Fail 7:1032–1041
11. Gao E, Lei YH, Shang X, Huang ZM, Zuo L, Boucher M, Fan Q, Chuprun JK, Ma XL, Koch WJ (2010) A novel and efficient model of coronary artery ligation and myocardial infarction in the mouse. Circ Res 107:1445–1453
12. Tsuda T, Gao E, Evangelisti L, Markova D, Ma X, Chu ML (2003) Post-ischemic myocardial fibrosis occurs independent of hemodynamic changes. Cardiovasc Res 59:926–933
13. He K, Chen X, Han C, Xu L, Zhang J, Zhang M, Xia Q (2014) Lipopolysaccharide-induced cross-tolerance against renal ischemia-reperfusion injury is mediated by hypoxia-inducible factor-2alpha-regulated nitric oxide production. Kidney Int 85:276–288
14. Matsui Y, Nakano N, Shao D, Gao S, Luo W, Hong C, Zhai P, Holle E, Yu X, Yabuta N, Tao W, Wagner T, Nojima H, Sadoshima J (2008) Lats2 is a negative regulator of myocyte size in the heart. Circ Res 103:1309–1318
15. Abbate A, Biondi-Zoccai GG, Baldi A (2002) Pathophysiologic role of myocardial apoptosis in post-infarction left ventricular remodeling. J Cell Physiol 193:145–153
16. Nishida K, Kaziro Y, Satoh T (1999) Anti-apoptotic function of Rac in hematopoietic cells. Oncogene 18:407–415
17. Frangogiannis NG (2006) The mechanistic basis of infarct healing. Antioxid Redox Signal 8:1907–1939
18. Chen W, Frangogiannis NG (2013) Fibroblasts in post-infarction inflammation and cardiac repair. Biochim Biophys Acta 1833:945–953
19. Ahn A, Frishman WH, Gutwein A, Passeri J, Nelson M (2008) Therapeutic angiogenesis: a new treatment approach for ischemic heart disease–part I. Cardiol Rev 16:163–171
20. Zhu H, Jiang X, Li X, Hu M, Wan W, Wen Y, He Y, Zheng X (2015) Intramyocardial delivery of VEGF via a novel biodegradable hydrogel induces angiogenesis and improves cardiac function after rat myocardial infarction. Heart Vessels. doi:10.1007/s00380-015-0710-0
21. Cohn JN, Ferrari R, Sharpe N (2000) Cardiac remodeling–concepts and clinical implications: a consensus paper from an international forum on cardiac remodeling. Behalf of an International Forum on Cardiac Remodeling. J Am Coll Cardiol 35:569–582
22. Willy PJ, Umesono K, Ong ES, Evans RM, Heyman RA, Mangelsdorf DJ (1995) LXR, a nuclear receptor that defines a distinct retinoid response pathway. Genes Dev 9:1033–1045
23. Zelcer N, Tontonoz P (2006) Liver X receptors as integrators of metabolic and inflammatory signaling. J Clin Invest 116:607–614
24. Wang Y, Li C, Cheng K, Zhang R, Narsinh K, Li S, Li X, Qin X, Zhang R, Li C, Su T, Chen J, Cao F (2014) Activation of liver X receptor improves viability of adipose-derived mesenchymal stem cells to attenuate myocardial ischemia injury through TLR4/NF-κB and Keap-1/Nrf-2 signaling pathways. Antioxid Redox Signal 21:2543–2557
25. Pelzer T, Loza PA, Hu K, Bayer B, Dienesch C, Calvillo L, Couse JF, Korach KS, Neyses L, Ertl G (2005) Increased mortality and aggravation of heart failure in estrogen receptor-beta knockout mice after myocardial infarction. Circulation 111:1492–1498
26. Tomaselli GF, Marban E (1999) Electrophysiological remodeling in hypertrophy and heart failure. Cardiovasc Res 42:270–283
27. White HD, Norris RM, Brown MA, Brandt PW, Whitlock RM, Wild CJ (1987) Left ventricular end-systolic volume as the major determinant of survival after recovery from myocardial infarction. Circulation 76:44–51
28. Gao F, Tao L, Yan W, Gao E, Liu HR, Lopez BL, Christopher TA, Ma XL (2004) Early anti-apoptosis treatment reduces myocardial infarct size after a prolonged reperfusion. Apoptosis 9:553–559
29. Sam F, Sawyer DB, Chang DL, Eberli FR, Ngoy S, Jain M, Amin J, Apstein CS, Colucci WS (2000) Progressive left ventricular remodeling and apoptosis late after myocardial infarction in mouse heart. Am J Physiol Heart Circ Physiol 279:H422–H428
30. Li HL, Zhuo ML, Wang D, Wang AB, Cai H, Sun LH, Yang Q, Huang Y, Wei YS, Liu PP, Liu DP, Liang CC (2007) Targeted cardiac overexpression of A20 improves left ventricular performance and reduces compensatory hypertrophy after myocardial infarction. Circulation 115:1885–1894
31. Manabe I, Shindo T, Nagai R (2002) Gene expression in fibroblasts and fibrosis: involvement in cardiac hypertrophy. Circ Res 91:1103–1113
32. Martos R, Baugh J, Ledwidge M, O'Loughlin C, Conlon C, Patle A, Donnelly SC, McDonald K (2007) Diastolic heart failure: evidence of increased myocardial collagen turnover linked to diastolic dysfunction. Circulation 115:888–895
33. Boyle AJ, Kelly DJ, Zhang Y, Cox AJ, Gow RM, Way K, Itescu S, Krum H, Gilbert RE (2005) Inhibition of protein kinase C reduces left ventricular fibrosis and dysfunction following myocardial infarction. J Mol Cell Cardiol 39:213–221
34. Heymans S, Luttun A, Nuyens D, Theilmeier G, Creemers E, Moons L, Dyspersin GD, Cleutjens JP, Shipley M, Angellilo A, Levi M, Nube O, Baker A, Keshet E, Lupu F, Herbert JM, Smits JF, Shapiro SD, Baes M, Borgers M, Collen D, Daemen MJ, Carmeliet P (1999) Inhibition of plasminogen activators or matrix metalloproteinases prevents cardiac rupture but impairs therapeutic angiogenesis and causes cardiac failure. Nat Med 5:1135–1142
35. Lee SH, Wolf PL, Escudero R, Deutsch R, Jamieson SW, Thistlethwaite PA (2000) Early expression of angiogenesis factors in acute myocardial ischemia and infarction. N Engl J Med 342:626–633
36. Spyridon M, Moraes LA, Jones CI, Sage T, Sasikumar P, Bucci G, Gibbins JM (2011) LXR as a novel antithrombotic target. Blood 117:5751–5761